Environmental Science Nano

ROYAL SOCIETY OF CHEMISTRY

PAPER

View Article Online
View Journal | View Issue

Cite this: *Environ. Sci.: Nano*, 2025, 12, 3329

Cellulose acetate-nanoMOF beads: a safe, sustainable and scalable solution for Pb remediation in complex water systems†

Prathmesh Bhadane [ab] and Swaroop Chakraborty *[a]

Received 16th January 2025,
Accepted 12th May 2025

DOI: 10.1039/d5en00056d

rsc.li/es-nano

Pb [Pb(II)] contamination poses a critical environmental and public health challenge, necessitating innovative and sustainable remediation strategies. This study presents cellulose acetate (CA)-BNMG-1 nanoMOF beads, synthesised *via* a green, water-based process without hazardous chemicals. By embedding this nanoMOF into a CA polymer matrix, the beads achieve remarkable Pb(II) removal efficiencies exceeding 80% in complex aqueous systems, including canal water and artificial seawater, even with competing ions and naturally occurring microbial contaminants in canal water. The beads exhibit significantly enhanced selectivity for Pb(II), with separation factors (SFs) improving from 2.5 to 350 for Pb/Mn, 57.4 to 220.6 for Pb/Ni, and 150.6 to 314 for Pb/Cd compared to the parent BNMG-1 nanoMOF. Structural stability is ensured, with Cu(II) leaching reduced to below 5% at higher and less than 1% at lower Pb(II) concentrations (5 bead per mL). Furthermore, the beads demonstrate outstanding reusability, retaining over 95% Pb(II) removal efficiency after three cycles. The CA matrix enhances nanoMOF stability, facilitating bead recovery *via* simple filtration, addressing challenges in scalability and sustainability. This work aligns with safe and sustainable by design (SSbD) framework, providing an eco-friendly and scalable solution for heavy metal remediation, advancing sustainable water treatment technologies for real-world applications.

Environmental significance

The developed cellulose acetate (CA)-BNMG-1 nanoMOF beads provide a scalable, eco-friendly, and effective solution for Pb (Pb(II)) remediation from complex aqueous environments, addressing a critical public health challenge. Synthesised *via* a green, water-based process, the beads reduce Cu(II) leaching to below 5%, ensuring environmental safety. Exceptional selectivity, with separation factors surpassing 350 for Pb(II) over competing ions, positions these beads as a transformative technology. Their mechanical robustness, ease of recovery, and high reusability (>95% efficiency after three cycles) highlight their potential for sustainable water treatment, aligning with global efforts to mitigate heavy metal pollution in water systems.

1. Introduction

Rapid industrialisation and the unethical disposal of industrial waste and untreated wastewater have caused significant damage to environmental water systems.[1,2] The direct discharge of untreated wastewater into active water streams poses severe health hazards to both humans and animals. Among the various pollutants, such as heavy metals, organic dyes, and pharmaceutical waste, heavy metal contamination stands out as a critical global issue.[3,4] Trace amounts of heavy metals have been detected in rivers worldwide, making their detection and removal a significant challenge.[5,6] Among these, heavy metals like arsenic, cadmium, nickel, and Pb are of particular concern due to their toxicity and persistence in the environment.[7] Lead (Pb), in particular, is one of the most toxic metals, widely used in applications such as batteries, alloys, pigments, paints, and energy storage systems.[8] Over time, Pb leaches into water primarily through the oxidation of Pb-containing materials, forming highly soluble Pb(II) ions in the presence of water and oxygen. Pb contamination in wastewater originates from various industrial activities, with concentrations varying depending on the source. Wastewater from battery manufacturing processes typically contains Pb concentrations ranging from 1 to 50 mg L^{-1}, while paint and pigment manufacturing contribute levels between 1 and 25 mg L^{-1}. Additionally, effluents from electroplating industries are known to contain Pb in the range of 8 to 10 mg L^{-1}. These

[a] *School of Geography, Earth & Environmental Sciences, University of Birmingham, Edgbaston, B15 2TT, UK. E-mail: s.chakraborty@bham.ac.uk*
[b] *Materials Engineering, Indian Institute of Technology, Gandhinagar, 382355, India*

† Electronic supplementary information (ESI) available. See DOI: https://doi.org/10.1039/d5en00056d

variations highlight the diverse and significant sources of Pb pollution, necessitating tailored remediation strategies for effective mitigation.[9]

Despite the urgent need for Pb remediation, developing a simple and effective strategy for the selective removal of Pb(II) ions from water remains a significant challenge. The presence of competing ions such as calcium, magnesium, and other transition metals often interferes with the selectivity and efficiency of existing removal techniques. Most conventional methods lack the precision required to isolate Pb ions without impacting water quality or leaving residual contaminants. There are reported studies where selective Pb removal has been achieved, particularly through adsorption-based methods.[10–14] For example, Aljohani, Majed S., *et al.* reported a cellulose-based bio-adsorbent for selective Pb(II) removal. In this study, cellulose was functionalised with 4-(2-pyridyl)thiosemicarbazide (PTC) hydrazidine to impart $-NH_2$ functional groups, resulting in a Pb(II)-imprinted adsorbent (Pb-PTC-CE). This ion imprinted porous structure showed high selectivity towards the Pb(II) ions.[15] Guo, Xuen, *et al.* developed a SiQD-nanoSiO_2-PVA composite film (SSP) that demonstrated dual functionality for Pb(II) removal and detection. The SSP composite exhibited a high adsorption capacity, exceptional selectivity, and reusability across five cycles, highlighting its practical potential in wastewater treatment.[16] However, many of these methods rely on adsorbents that involve complex and time-consuming synthesis procedures, require extensive post-processing, or depend on expensive and non-sustainable materials. These challenges limit their scalability and practical applicability for large-scale water treatment systems. In this context, safe and sustainable by design (SSbD) framework[17] has garnered attention for integrating performance with safety and sustainability criteria, ensuring minimal environmental impact across the material's lifecycle.[18,19] Recent advancements highlight the importance of adopting green chemistry approaches and eco-friendly synthesis methods, reducing reliance on hazardous chemicals and energy-intensive processes.[20] Such an approach aligns with global efforts to advance green technologies for water treatment.[21]

Developing a cost-effective, environmentally friendly, and efficient adsorbent for selective heavy metal removal remains a critical research priority. In this context, metal–organic frameworks (MOFs) have emerged as a promising class of materials for addressing the challenges of heavy metal removal.[22,23] MOFs are highly porous, crystalline structures composed of metal nodes and organic linkers, offering exceptional surface area, tuneable functionality, and structural flexibility. Their unique properties make them ideal candidates for adsorption-based applications, including the selective removal of Pb(II) from water. Furthermore, the ability to modify MOFs at the molecular level as well as possible external modifications enables precise control over their chemical affinity and selectivity, making them a versatile platform for water purification technologies.[24]

However, despite their many advantages, conventional MOFs face significant challenges in aqueous systems, primarily due to their instability.[25] Prolonged exposure to water often results in structural degradation and diminished adsorption efficiency. For instance, well established HKUST-1 MOF, which remains stable in water for only up to 2 hours, poses challenges for practical scalability. Improving its stability necessitates additional modifications such as post-functionalization or doping.[26] Additionally, separating MOF powders from aqueous solutions after adsorption is both complex and inefficient, limiting their practicality for continuous water treatment applications.[27] Another critical issue, often overlooked, is the leaching of metal ions during MOF applications, which raises environmental and performance concerns.[28] Furthermore, complex synthesis methods, high preparation costs, and the use of toxic chemicals hinder their large-scale applicability.[29] In a recent study, Zhi, Gang, *et al.* employed an *in situ* synthesis method to fabricate nylon foam-MOF composites for selective arsenic (As) removal from smelting wastewater.[30] However, the synthesis process required intricate hydrothermal conditions and precise control of precursor concentrations, posing challenges for scalability and raising questions about cost-effectiveness and the environmental impact of large-scale production.

To overcome these issues, our study reported nanoMOF-based monoliths by incorporating BNMG-1 nanoMOF into cellulose acetate (CA) polymer beads. BNMG-1 MOF, synthesised in a single-step, one-pot process within 30 minutes without the need for post-processing, exhibits exceptional adsorption capacity for heavy metal ions (Pb, Cd, Mn, and Ni) and rare earth elements (Y and Nd). It was incorporated as a reinforcement into a CA matrix. However, separating the MOF from contaminated aqueous system after adsorption is challenging, and approximately 20% Cu(II) leaching into water was observed during heavy metal and REE adsorption.[31,32] The preparation of CA-BNMG-1 composite beads aligns with SSbD framework by enhancing the MOF's stability in aqueous environments and enabling efficient adsorbent recovery without energy-intensive separation processes. These composite beads combine the high adsorption capacity and selectivity of MOFs with the mechanical robustness and processability of CA, offering a scalable, safe, and environmentally sustainable solution for selective Pb removal from contaminated water. This work, promotes the cross material[33] synergy by forming polymer MOF composite.

2. Materials and methods

2.1. Materials section

Cellulose acetate [Mn 50 000 by GPC, Sigma Aldrich], copper nitrate trihydrate (Cu $(NO_3)_2{\cdot}3H_2O$) [Sigma Aldrich], 2-methylimidazole (2-MeIM) [Sigma Aldrich], Pb nitrate [Sigma Aldrich-MW: 331.2 g mol^{-1}], dimethyl sulfoxide (DMSO) [Sigma Aldrich].

2.2. Synthesis and characterisation of BNMG-1 nanoMOFs, CA and CA-BNMG-1 beads

The BNMG-1 nanoMOF was synthesised (Section S1†) using a previously reported method,[31] ensuring phase purity and

structural integrity. CA beads were synthesised using a phase separation technique. For this, 1 g of CA was dissolved in 10 mL of DMSO. To prepare CA-BNMG-1 composite beads, 20 wt% of BNMG-1 MOF was uniformly dispersed in the CA-DMSO solution prior to extrusion, ensuring homogeneous MOF distribution within the polymer matrix. Both the CA and CA-BNMG-1 solutions were then extruded dropwise into ultrapure water using a 5 mL syringe to form beads. The resulting beads were thoroughly washed with ultrapure water to remove any residual DMSO and then dried at 37 °C in an oven.

The synthesised BNMG-1, CA and CA-BNMG-1 beads were extensively characterised to confirm their structure, morphology, and composition. Phase identification was conducted using X-ray diffraction (XRD) on a Bruker D8-XRD instrument (Cu-Kα radiation) over a 2θ range of 5–50°. The morphology and size of the BNMG-1 nanoMOF, as well as the surface and cross-sectional features of the beads, were examined using scanning electron microscopy (SEM-JEOL JSM7900F) and transmission electron microscopy (TEM-FEI, Themis). Energy-dispersive X-ray spectroscopy (EDS) verified the uniform incorporation of BNMG-1 within the CA-BNMG-1 composite beads. Fourier transform infrared spectroscopy (FTIR, Spectrum Perkin Elmer, USA) in the range of 400–4000 cm^{-1} was employed to confirm the molecular bonds and functional groups characteristic of BNMG-1 and its integration into the composite beads. Thermal stability was analysed using thermogravimetric analysis (TGA-Perkin Elmer 4000) from 30 °C to 500 °C at a heating rate of 10 °C per minute. The copper [Cu(II)] content in both the BNMG-1 MOF and CA-BNMG-1 beads was quantified using inductively coupled plasma mass spectrometry (ICP-MS, Nexion 350, Perkin Elmer, USA) following complete acid digestion using ashing mixture (3 : 1 Molar ratio of HNO_3 and H_2O_2 under heating at 120 °C).[34]

2.3. Pb(II) removal studies in multi-component aqueous systems

The removal of Pb from water using prepared composite beads was systematically studied to elucidate the underlying kinetics and mechanism. Kinetic studies were conducted by treating a 10 mg L^{-1} Pb solution prepared using Pb nitrate and ultrapure water. This solution was treated using 5 beads per mL at varying time intervals (0, 0.5, 1, 3, 6, 24, and 48 hours), enabling an evaluation of removal rates and equilibrium dynamics. To determine the removal capacity of composite beads, isotherm studies were performed with Pb solutions spanning a concentration range of 10–1000 mg L^{-1}. These experiments used a single composite bead per 1 mL of solution to accurately profile removal behaviour across diverse concentration levels. The effect of bead quantity on removal efficiency was also examined by varying the number of beads (1, 5, 10, and 20 beads per mL). The reusability of the composite beads was assessed over multiple removal cycles using a 10 mg L^{-1} Pb solution, providing insights into their operational stability and performance. These detailed analyses offered critical insights into the kinetics, capacity, and mechanism of Pb removal, emphasising the potential of CA-BNMG-1 composite beads as a highly effective material for water purification and Pb remediation in environmental applications.

The selectivity of CA-BNMG-1 composite beads for Pb(II) were evaluated under complex aqueous conditions to simulate realistic environmental scenarios. Two types of systems were used for these studies, where these systems were treated with CA-BNMG-1 beads for 24 h.

Mixture of heavy metal ions. A multi-metal solution containing Mn(II), Ni(II), Cd(II), and Pb(II), each at an initial concentration of 40 mg L^{-1}, was prepared using their respective salts to evaluate the competitive adsorption behaviour of the composite beads. The solution pH was adjusted to 5 and subsequently treated with the prepared composite beads for 24 h under continuous agitation in an incubator shaker at 25 °C. Post-treatment, the supernatant was collected, and the residual metal ion concentrations were analysed to determine the beads' preferential binding affinity toward Pb(II) in the presence of competing ions. Using eqn (S3) and (S4),† distribution coefficient (K_d) and separation factor (SF) were calculated.

Complex water matrix systems. The beads were tested in two additional conditions: canal water (CW) collected from Birmingham Canal (collected from Birmingham Canal near Selly Oak Railway Bridge, Birmingham, UK, details in Section S3†), UK spiked with 10 mg L^{-1} Pb(II) and artificial seawater (ASW) (Section S3†) spiked with 10 mg L^{-1} Pb(II). These scenarios were chosen to explore the beads' performance in matrices with varying ionic strengths and potential organic and inorganic contaminants [1 bead per mL, denoted as CW-1 and ASW-1 for canal water and artificial seawater, respectively, 5 beads per mL, denoted as CW-5 and ASW-5].

Following the removal process in each study, aliquots of the treated solutions were collected, diluted using 2% nitric acid, and analysed using ICP-MS (in KED mode, helium 4 mL min^{-1}, dwell time – 50 ms) to measure residual Pb(II) concentrations and the release of Cu(II) ions from the composite beads in aqueous solution. The kinetic data were modelled using pseudo-first-order and pseudo-second-order equations to determine the dominant removal mechanism. Similarly, isotherm data were analysed using the Langmuir and Freundlich models to characterise surface interaction homogeneity and removal coverage. All experiments were conducted in triplicate to calculate the standard deviation and assess the reproducibility of the results.

2.4. Post adsorption analysis

To assess potential structural changes and the adsorption mechanism of Pb(II) on composite beads, XRD, SEM-EDS, XPS, and FTIR analyses were performed both before and after Pb(II) adsorption. The chemical composition of the composite beads before and after Pb(II) adsorption was analyzed using X-ray photoelectron spectroscopy (XPS; K-Alpha, Thermo Fisher Scientific) with an Al-Kα radiation source (energy =

1486.6 eV). Survey spectra were acquired at a pass energy of 200 eV with a step size of 1 eV, while high-resolution spectra for Pb 4f, N 1s, and O 1s were recorded at a pass energy of 50 eV with a step size of 0.1 eV. The obtained spectra were deconvoluted and fitted using CasaXPS with Gaussian–Lorentzian functions and a Shirley background. The C 1s peak at 284.6 eV was used as the binding energy reference for all spectra. These techniques provided insights into any modifications in the crystalline structure, functional groups, and surface chemistry of CA-BNMG-1 beads resulting from interaction with Pb(II).

3. Results and discussion

The BNMG-1 nanoMOF exhibits a unique two-dimensional sheet-like structure, as revealed by SEM and TEM micrographs [Fig. 1(A and B)]. These nanosheets are randomly contoured, with a smooth surface and thickness less than 20 nm. Their lateral dimensions range between 250 and 500 nm, and their shape reflects a natural irregularity, contributing to their distinct morphology. The nanosheets maintain structural uniformity at the nanoscale, which is crucial for their functional properties. The incorporation of BNMG-1 into CA beads was confirmed by multiple characterisation techniques. SEM micrographs of composite beads [Fig. 1(D–F)] displayed a highly porous structure, indicative of their potential for high MOF loading capacity and enhanced material interactions. The presence of BNMG-1 MOF nanosheets embedded within the CA matrix and porous structure of composite beads was also confirmed using cross sectional SEM and EDX analysis [Fig. 1F and S1 and Table S1†]. FTIR analysis (Fig. S2†) of BNMG-1 revealed distinct peaks for the 2-MeIM linker, including 1423 cm^{-1} and 1307 cm^{-1} for C–N stretching, 1150 cm^{-1} for C–H stretching, and strong bands at 1570 cm^{-1} and 1618 cm^{-1} for –C═N stretching. An absorption band at 431 cm^{-1} confirmed the Cu–N bond, validating the coordination between copper and the linker.[35] In CA beads, key peaks at 1737 cm^{-1} (C═O stretching), 1440 cm^{-1} (H–C–H vibrations), and 1215 cm^{-1} (C–O stretching) highlighted ester linkages. Missing peaks and increased intensity in some bands suggested interactions between CA and BNMG-1, supported by a broad peak at 3650 cm^{-1} associated with O–H and N–H stretching.

Thermal analysis through TGA (Fig. S3†) revealed BNMG-1's three-stage degradation: stability up to 240 °C, a 25% mass loss around 250 °C due to free 2-MeIM ligands, and gradual decomposition of coordinated 2-MeIM up to 500 °C. The CA-BNMG-1 composite exhibited a slightly earlier onset of degradation due to interactions between CA and BNMG-1. A significant mass loss around 360 °C was attributed to CA decomposition, consistent with DTG findings (Fig. 1C). XRD pattern (Fig. 1G) showed characteristic peaks for BNMG-1 at 14.7°, 29.8°, 33.2°, and 47.7°, confirming its crystalline nature and purity. These peaks persisted in the CA-BNMG-1 composite, along with a broad hump around 22.5° from the amorphous cellulose acetate.[36] The CA-BNMG-1 beads retained MOFs characteristic peaks in both FTIR and XRD spectra, indicating its structural stability within the CA matrix. Elemental composition measured by ICP-MS showed that each composite bead (2.5–3 mg) contained approximately 0.72 mg of MOF, representing 20–30 wt% of the composite mass. This wt% matched the initial synthesis composition and indicated minimal loss during preparation. These analyses confirm the successful integration of BNMG-1 into the CA matrix, preserving the MOF's characteristic morphology and structural integrity. The observed compatibility and synergistic interactions between

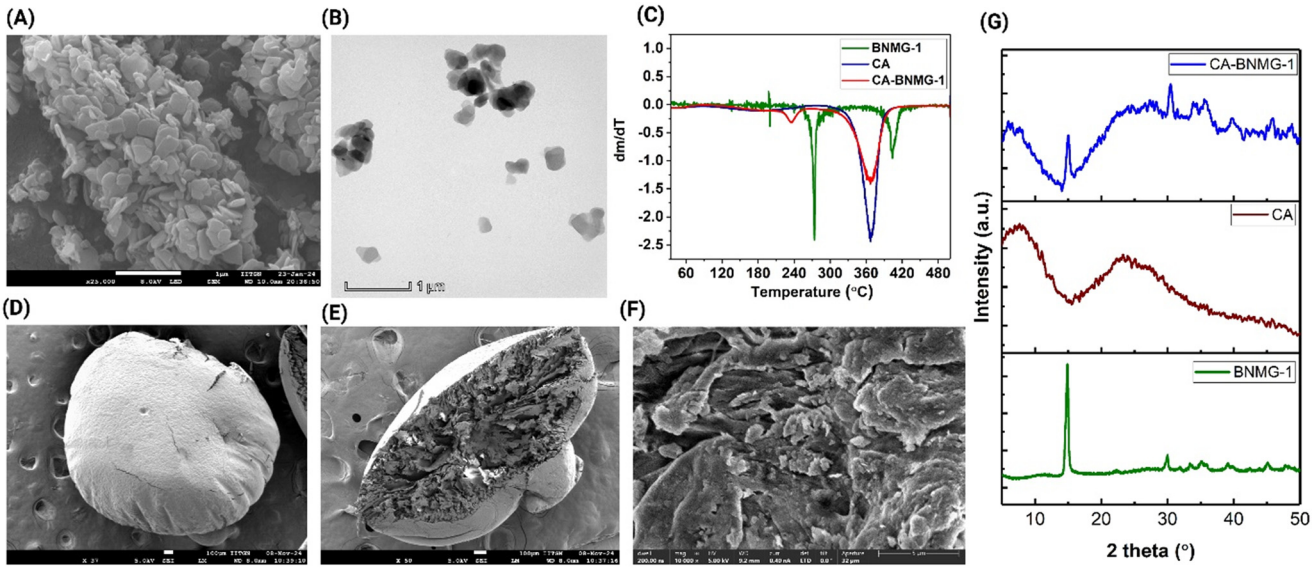

Fig. 1 Characterisation of prepared BNMG-1 nanoMOF, CA and CA-BNMG-1 composite beads (A and B) SEM and TEM micrograph of BNMG-1 MOF (C) comparative derivative thermogravimetric (DTG) curves (D–F) topography and cross-sectional SEM micrograph of composite beads and (G) X-ray diffraction pattern of BNMG-1, CA and CA-BNMG-1 composite beads.

the two materials enhance the composite's structural and functional properties, establishing a strong foundation for its potential in environmental remediation applications.

The effect of adsorbent contact time with Pb(II) ions plays a significant role in understanding the removal kinetics when using CA-BNMG-1 beads. It was observed that Pb(II) removal was rapid, achieving more than 90% removal efficiency (RE) [eqn (S1)†] within the first 30 minutes of contact time (Fig. 2A). This high initial removal rate can be attributed to the availability of abundant O and N active sites on the surface, the larger surface area and porosity provided by the CA-BNMG-1 composite. As contact time increased, the RE value continued to improve slightly, reaching an equilibrium RE of 98%. The equilibrium removal capacity (Q_e) of CA-BNMG-1 beads for Pb(II) was determined to be 0.82 mg g^{-1} (eqn (S2)†) based on experimental analysis. Kinetic model fitting was done using pseudo-first order (PFO) (eqn (S5), Fig. S4†) and pseudo-second-order (PSO) (eqn (S6),† Fig. 2B). It was observed that the removal process adhered closely to the PSO model, as evidenced by a regression coefficient (R^2) of 0.9993 and Q_e of 0.807 mg g^{-1}. It suggests that chemisorption is the dominant mechanism driving Pb(II) removal (Table S1†). The system achieved Pb(II) removal equilibrium within 3 hours, with minimal Cu(II) leaching, less than 1% into the water (Fig. 2C). The rapid removal rate and excellent alignment with the PSO model highlight the high efficiency of CA-BNMG-1 beads for Pb(II) adsorption. To confirm the affinity of Pb(II) towards composite beads distribution coefficient values were also calculated using eqn (S3).† The obtained K_d values (5.7×10^5 mL g^{-1}) in the range of 10^5 indicate a strong affinity of composite beads for Pb(II) and The rise in log K_d with increasing adsorbent dosage is attributed to the greater availability of adsorption sites at higher concentrations (Fig. 2D). An adsorbent is generally considered excellent when K_d exceeds the threshold value of 10^5 mL g^{-1}.[37]

The maximum adsorption capacity of Pb(II) by CA-BNMG-1 beads and Cu(II) leaching from beads was evaluated using batch adsorption isotherm experiments [Fig. 3(A and B)]. Langmuir (eqn (S7),† Fig. 3B) and Freundlich (eqn (S8), Fig. S5†) models were applied to describe the adsorption process, with the Langmuir model providing a better fit (R^2 = 0.9510) (Table S2†). This suggests that adsorption primarily occurs as a monolayer on the surface of the beads, with a maximum adsorption capacity of 24.9 mg g^{-1} for CA-BNMG-1 beads. Meanwhile, Cu(II) leaching increased gradually from less than 1% at 1 mg L^{-1} to up to 4% in a highly concentrated system of 1000 mg L^{-1} (Fig. 3C). The Fig. 3D illustrates the

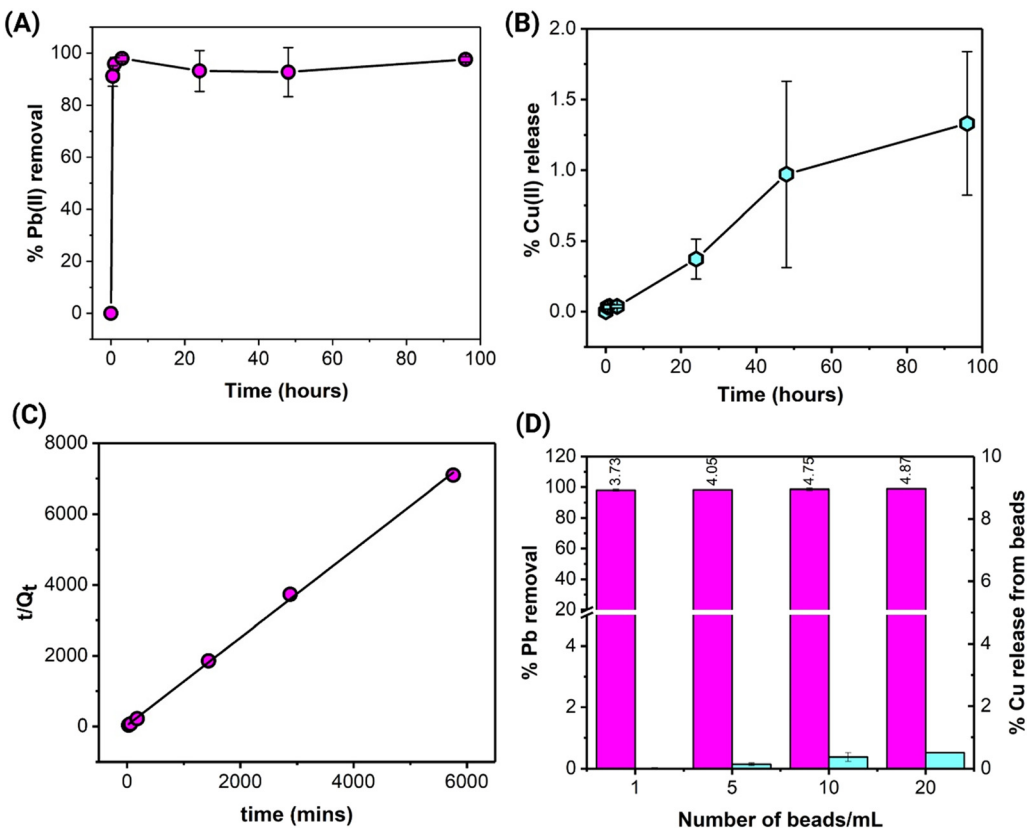

Fig. 2 Batch adsorption experiments. (A) Kinetic adsorption study [10 mg L^{-1} Pb(II), 5 beads per mL]. (B) Cu(II) release during the adsorption kinetics. (C) Pseudo second order kinetics model fitting. (D) Effect of bead quantity variation on Pb(II) removal and Cu(II) leaching with log k_d [coefficient of distribution (K_d)] value labelled calculated using equation eqn (S3).† All experiments were conducted in triplicate to calculate the standard deviation and assess the reproducibility of the results.

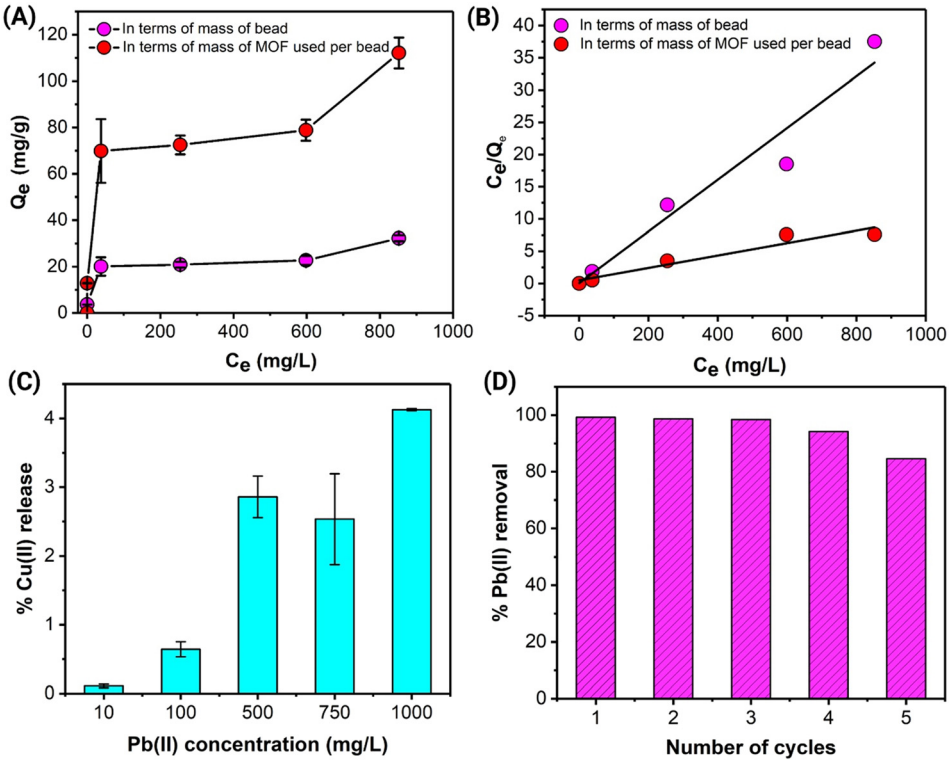

Fig. 3 Adsorption isotherm and reusability study: (A) adsorption isotherm study conducted with Pb(II) concentrations ranging from 10 to 1000 mg L^{-1} [1 bead per mL], with adsorption capacity reported based on both bead mass and the MOF content per bead. (B) Langmuir isotherm model fitting for Pb(II) adsorption. (C) Cu(II) release during the adsorption isotherm study. (D) Reusability assessment of the prepared beads for Pb(II) removal [10 mg L^{-1}, 5 beads per mL, 6 hours]. All experiments were conducted in triplicate to calculate the standard deviation and assess the reproducibility of the results.

reusability of CA-BNMG-1 beads over multiple adsorption–desorption cycles. The beads retained their high Pb(II) removal efficiency, achieving over 95% removal even after three consecutive cycles, demonstrating their robust performance and reusability. When considering only the BNMG-1 MOF content, the maximum adsorption capacity was 86.45 mg g^{-1}, while the experimental value for BNMG-1 was 112.1 mg g^{-1}. While this value is lower than the direct use of BNMG-1 powder for Pb(II) adsorption, the bead format offers significant practical advantages by addressing three critical challenges associated with the direct use of BNMG-1 MOF:

Leaching control: direct use of MOF powder resulted in significant Cu(II) leaching, approximately 20%. In contrast, composite beads reduced this leaching to less than 5%, ensuring the structural stability of the MOF in aqueous systems.

Ease of separation: the bead format eliminates the need for labour-intensive or energy-intensive separation techniques like centrifugation or magnetic recovery. With a spherical size of 2–3 mm, the beads can be easily retrieved using simple mesh filtration.

Selectivity and reusability: the bead formulation enhances selectivity for Pb(II) even in the presence of competing metal ions, ensuring efficient performance in complex aqueous systems.

In experimental trials, 99.7% of Pb(II) from a 10 mg L^{-1} solution was adsorbed within 3 hours using a dosage of 5 beads per mL. Despite a slightly lower maximum adsorption capacity compared to the MOF powder, the composite beads offer a sustainable solution by mitigating Cu(II) leaching and simplifying recovery processes. Apart from this, as highlighted in the introduction, Pb contamination in wastewater typically falls within the range of 1–50 mg L^{-1}. The CA-BNMG-1 beads demonstrate remarkable efficiency in effectively removing Pb within this concentration range, displaying their potential as a robust remediation solution.

The selectivity tests conducted in various complex aqueous systems demonstrated the superior ability of these beads to selectively capture Pb(II) even in the presence of coexisting ions. As depicted in the Fig. 4A and corroborated by our previously published work,[31] while the parent BNMG-1 MOF exhibits broad-spectrum adsorption of multiple heavy metal ions, the CA-BNMG-1 beads stand out for their exceptional selectivity toward Pb(II). For instance, as shown in Fig. 4(B and C), the separation factor (SF) of Pb relative to Mn [SF(Pb/Mn)] improved from 2.5 for BNMG-1 to an impressive 350 for CA-BNMG-1 beads, a remarkable 140-fold enhancement. Similarly, SF(Pb/Ni) and SF(Pb/Cd), which were 57.4 and 150.6 for BNMG-1, respectively, increased to 220.6 and 314 for the beads, showing nearly 4-fold and 2-fold improvements. This substantial enhancement in selectivity

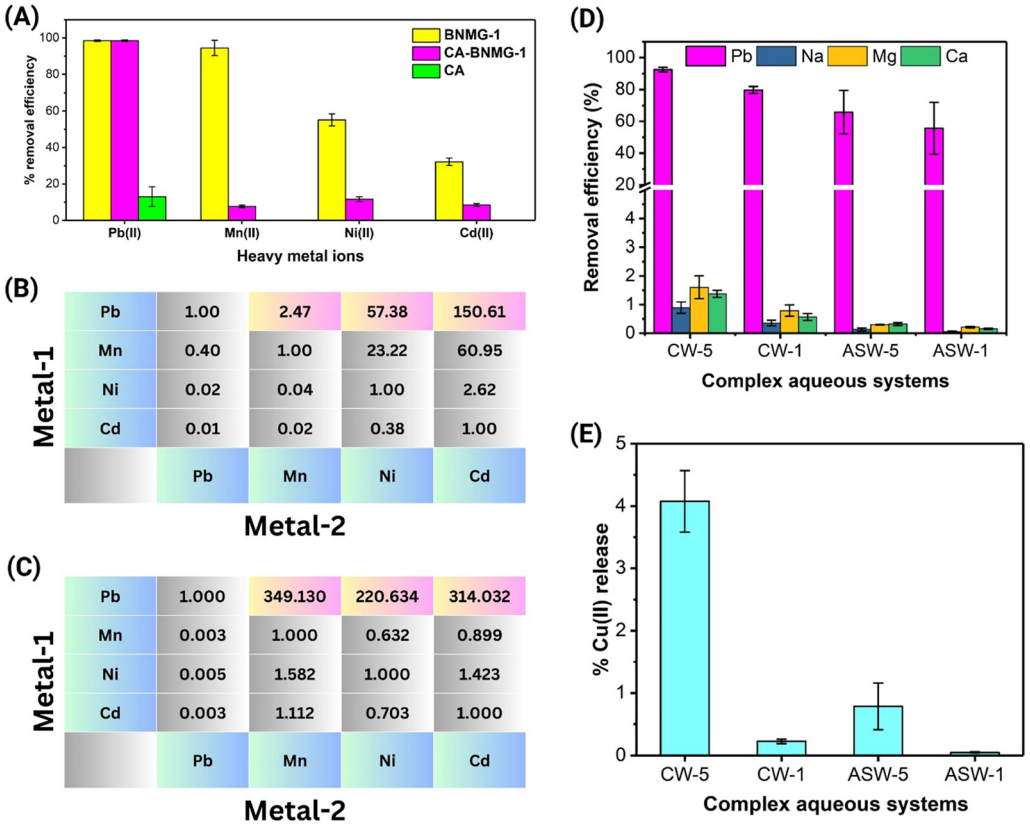

Fig. 4 Pb(II) removal from complex aqueous systems: (A) influence of competing metal ions on Pb(II) removal from a complex mixture containing Pb(II), Mn(II), Ni(II), and Cd(II) using pristine BNMG-1 powder, CA beads, and CA-BNMG-1 composite beads. (B and C) Separation factor (SF) calculated using eqn (S4),† illustrating the affinity of BNMG-1 and CA-BNMG-1 for different metal ions. (D) Pb(II) removal performance of the composite beads in canal water and artificial seawater (ASW) [5 beads per 2 mL, 24 hours]. (E) Cu(II) leaching from the beads during Pb(II) adsorption experiments in canal water and ASW. All experiments were conducted in triplicate to calculate the standard deviation and assess the reproducibility of the results.

can be attributed to the confined adsorption sites within the CA-BNMG-1 beads. These sites exhibit a strong preference for Pb(II), which has a higher distribution coefficient compared to other metal ions. Consequently, Pb(II) occupies the active sites preferentially, leaving limited opportunities for other ions to bind. In contrast, the bare BNMG-1 MOF contains a larger number of adsorption sites, allowing co-adsorption of multiple ions even after Pb(II) binding. This explains the beads' highly selective Pb(II) adsorption behavior in competitive environments.

The affinity of CA-BNMG-1 beads toward Pb(II) was further validated in a spiked Pb-contaminated canal water (CW) and artificial sea water (ASW) systems, as shown in the Fig. 4D. Even in such complex aqueous environments, containing diverse anions, cations, and naturally occurring microbial contaminants, the CA-BNMG-1 beads demonstrated exceptional selectivity for Pb(II) removal. Specifically, with a dosage of 5 beads per mL, the beads achieved more than 75% Pb(II) removal while releasing less than 5% Cu(II) (Fig. 4E). Remarkably, at a reduced dosage of 1 bead per mL, Pb(II) removal efficiency remained consistent at over 75%, with Cu(II) release dropping to below 1%. Furthermore, the adsorption of other coexisting ions, such as Na(I), Mg(II), and Ca(II), remained below 2%, ensuring minimal interference with the ion composition essential for a healthy water system.

Similar trends were observed in ASW shown in Fig. 4(D and E), where the CA-BNMG-1 beads achieved approximately 70% Pb(II) removal while maintaining negligible adsorption (less than 1%) of competing ions. These findings highlights the exceptional performance and high selectivity of the CA-BNMG-1 beads for Pb(II) even in highly competitive and realistic conditions. This selective behaviour, combined with minimal leaching of Cu(II), highlights the potential of CA-BNMG-1 beads as a robust and sustainable solution for the remediation of Pb(II)-contaminated water systems, ensuring both efficiency and environmental safety. These experiments provided a comprehensive understanding of the beads' selectivity for Pb(II) in the presence of other competing ions and under varying water chemistries, including high salinity environments. The results demonstrated the potential of CA-BNMG-1 composite beads for effective Pb removal from complex and diverse water systems, highlighting their applicability for environmental remediation.

The stability of the beads and adsorption mechanism was further validated through post-adsorption XRD, SEM-EDX, FTIR and XPS analysis, which revealed that structural

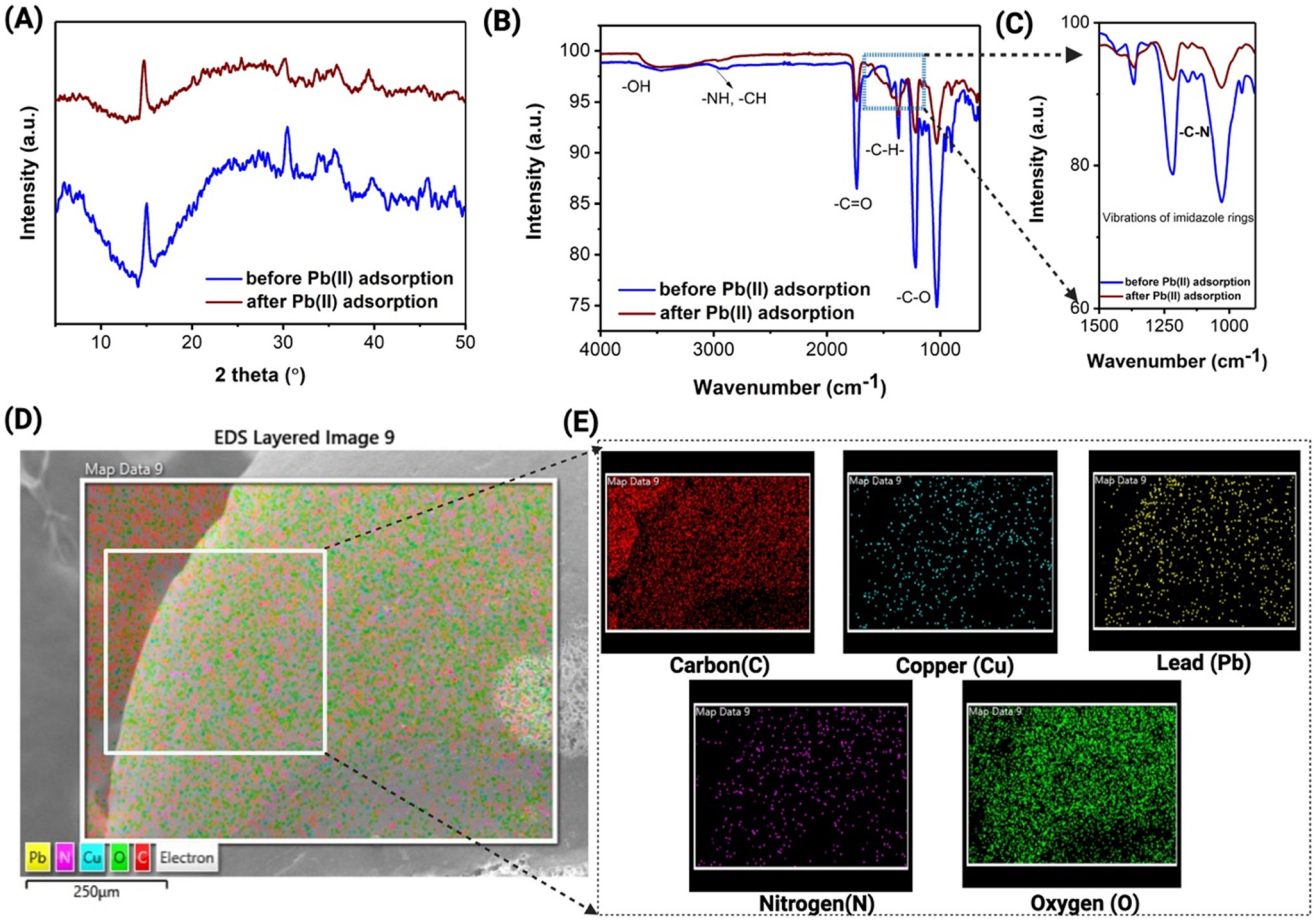

Fig. 5 Post adsorption analysis of composite beads and after Pb(II) adsorption: (A) post adsorption XRD pattern, (B and C) FTIR spectra of BNMG-1, CA and CA-BNMG-1 bead (D and E) elemental mapping of Pb(II) adsorbed composite bead.

integrity and crystallinity of MOF within bead remained intact after Pb(II) adsorption, as illustrated in the Fig. 5(A). All the distinct peaks of BNMG-1 were present after adsorption process. FTIR spectra presented in Fig. 5(B and C) provide insights into the adsorption mechanism, revealing that Pb(II) ions interact with the beads through groups containing nitrogen (N) in the 2-MeIM ligand of the BNMG-1 MOF. These groups serve as active sites for Pb(II) adsorption onto the CA-BNMG-1 beads. Shift and reduced intensity in peaks near 1200–900 cm^{-1} (stretching vibrations of 2-MeIM) after adsorption of Pb(II) confirms the involvement of functional group containing N.[38] Further, there is slight shift in the characteristic peak of CA (–C–O) was observed indicating possible interaction of Pb(II) with O present in beads. This complex interplay of interactions highlights the multifaceted nature of Pb adsorption on this composite beads, involving both oxygen and nitrogen coordination sites. EDS elemental mapping shown in Fig. 5D also confirmed the adsorption of Pb(II) on the surface of beads as well as into the pores of beads. To further confirm the interactions, XPS analysis was performed before and after the Pb(II) adsorption. XPS survey spectra (Fig. 6A) after adsorption of Pb(II) showed presence of characteristic Pb 4f peaks confirming adsorption of Pb(II). Deconvoluted XPS spectra of Pb 4f (Fig. 6B) showed peaks at binding energy (BE) 138.24 eV and 143.09 eV of Pb 4f7/2 and Pb 4f5/2 respectively. Characteristic deconvoluted peaks of $Pb(NO_3)_2$ comes around the 139.6 and 144.5 eV. This shift in BE to lower side shows the affinity of Pb(II) towards prepared composite beads.[39] The O 1s spectra of the CA-BNMG-1 beads, both before and after Pb(II) adsorption, are shown in Fig. 6(C and D). Prior to adsorption, the O 1s spectrum was deconvoluted into four distinct peaks corresponding to C═O, C–O–C, C–OH, and –OH groups. Where to C═O, C–O–C, and C–OH are characteristic peaks of cellulose acetate matrix.[40] Following Pb(II) adsorption, an overall increase in O 1s intensity was observed, along with the appearance of a new peak at 530.9 eV, which is attributed to Pb–O interactions. This suggests that Pb(II) adsorption onto the CA-BNMG-1 beads involves coordination with oxygen-containing functional groups. These findings align with the FTIR results, further supporting the adsorption mechanism. The XPS spectra of N 1s for the CA-BNMG-1 beads exhibit two peaks at binding energies of 398.39 eV and 399.6 eV, corresponding to the –N═ (imine) and –NH– (amine) groups of the imidazole ligand, respectively. After Pb(II) adsorption, the intensity of the –NH– peak decreases,

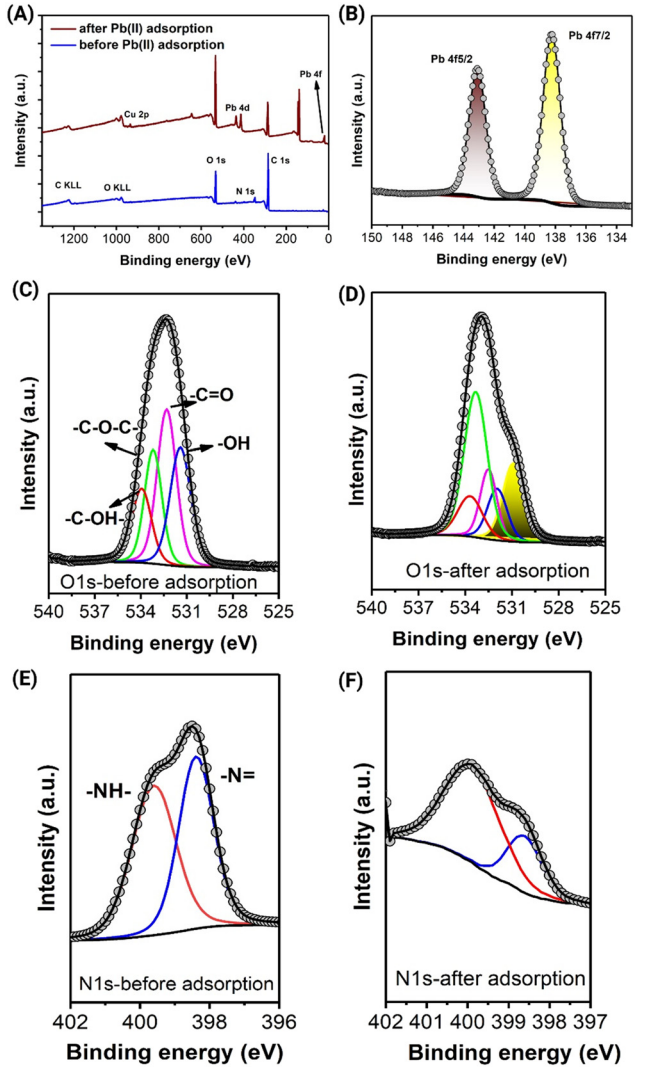

Fig. 6 (A) XPS survey spectra of CA-BNMG-1 beads before and after Pb(II) adsorption. (B–F) High-resolution spectra with deconvolution: (B) Pb 4f after adsorption, (C) O 1s before adsorption, (D) O 1s after adsorption, (E) N 1s before adsorption, and (F) N 1s after adsorption.

and a new peak emerges at 400.1 eV, indicating the coordination of protonated nitrogen (–N=$^{+}$) with the adsorbed Pb(II) ions. The drop in intensity of the N 1s peak in XPS spectra after Pb adsorption may indicate that these nitrogen atoms are shielded or involved in strong interactions with Pb, reducing their detectability by XPS. However, this decrease in intensity does not imply instability of the MOF framework. Notably, our previous work, which employed XPS analysis to elucidate the adsorption mechanism of Pb(II) onto BNMG-1, corroborates the findings of this study, confirming that a similar adsorption process occurred.[31]

Similar adsorption mechanism was reported by Nonkumwong, *et al.* where amine treated magnesium ferrite was used for the removal of Pb(II) from wastewater.[41] Overall, the enhanced stability, minimal Cu(II) leaching, and strong selectivity for Pb(II) can be attributed to the synergistic interplay between the BNMG-1 MOF and the CA matrix. The beads active sites (–O–, and –N–) provide robust Pb(II) adsorption through coordination interactions, while the CA matrix ensures structural integrity and prevents significant Cu(II) release.

The adsorption performance of the CA-BNMG-1 composite beads was compared with other reported adsorbents, such as coconut-shell carbon (CSC), activated carbon derived from European Black pine cones, and oxidized multi-walled carbon nanotubes (o-MWCNTs). Sekar *et al.* reported a maximum Pb(II) adsorption capacity of 26.50 mg g^{-1} for CSC at pH 4.5, while Momčilović *et al.* found that European Black pine-derived activated carbon achieved 27.53 mg g^{-1}, following the Langmuir isotherm model.[42,43] Additionally, Lasheen *et al.* reported that o-MWCNTs exhibited a Pb(II) adsorption capacity of 75 mg g^{-1}.[44] In comparison, the CA-BNMG-1 composite demonstrated significantly higher Pb(II) removal efficiency and adsorption capacity of 112 mg g^{-1} in terms of MOF used per bead, emphasizing its superior adsorption performance and potential for Pb remediation in complex aqueous systems. In addition, prepared composite beads align with safe-by-design goals and sustainability goals by integrating green chemistry, economic viability, environmental safety, and ease of use. Their water-based synthesis eliminates harmful organic solvents, ensuring resource efficiency and minimizing environmental impact. By embedding BNMG-1 MOFs into a biodegradable cellulose acetate matrix, the beads significantly reduce Cu(II) leaching by a factor of 20, with less than 1% Cu release in 24 hours compared to ~20% from bare BNMG-1. This stabilization enhances their long-term applicability in Pb(II) removal while maintaining environmental safety. The beads also demonstrate strong economic feasibility, with a cost-effective preparation process where laboratory-scale production cost of 2.88 GBP for 400 mg of BNMG-1 (£7.20 per g) and 3.78 GBP for 1–1.2 g of CA-BNMG-1 beads (£3.44 per g), making them scalable for large-scale water treatment applications. Their millimeter-sized structure facilitates easy separation *via* simple filtration methods, eliminating the need for complex recovery steps required for fine powders and reducing operational complexity. Moreover, the CA-BNMG-1 beads exhibit high selectivity for Pb(II) even in complex aqueous environments, efficiently removing Pb despite the presence of competing ions. This selective adsorption, coupled with their stability and scalability, highlights their potential for sustainable environmental remediation.

4. Outlook

The CA-BNMG-1 beads represent a sustainable and efficient solution for Pb(II) remediation, aligning with the SSbD framework.[17,45] Synthesised through a greener and rapid process using water as the sole solvent, the fabrication of BNMG-1 nanoMOF and its subsequent incorporation into cellulose acetate require no additional post-processing steps, minimizing energy and chemical consumption. The use of CA as a matrix material not only stabilises the nanoMOF but

Table 1 Effects of co-existing organics on Pb(II) removal efficiency

Organic compounds	Adsorbent/matrix	Environmental condition	Effect on Pb(II) removal	Key findings/mechanism	Ref.
Humic acid (HA)	MMSP-GO composite	pH 2–9, 20 mg L^{-1} Pb(II)	Enhancement at pH > 3	HA increased Pb(II) adsorption at neutral pH; likely due to electrostatic attraction and ternary complexation	46
Surfactants (anionic/cationic)	Modified biosorbents, activated carbon	pH variable, metal ions	Variable (depends on surfactant type)	Anionic surfactants can enhance Pb(II) adsorption; cationic surfactants may not improve or can inhibit	47
Humic acid (HA)	Lignocellulose-derived hydrothermal humic acid	pH 1–6, variable Pb(II)	Variable (depends on HA type)	Pore structure and oxygen content of HA are key; higher surface area and O-content improve Pb(II) adsorption	48
Surfactant (CTAB, cationic)	Microplastics-sediment complexes	CTAB 0–50 mg L^{-1}	Inhibition or enhancement (w/FA)	CTAB generally reduced Pb(II) adsorption, but with fulvic acid (FA), CTAB promoted Pb(II) adsorption	49
Natural organic matter (NOM) + microbes	CA-BNMG-1 beads	Canal water, artificial sea water, pH: 4–6, variable Pb(II) 1 to 100 mg L^{-1}	No significant difference	Pb(II) removal efficiency consistent in canal water (with NOM/microbes) and synthetic solutions; organics unquantified	This work

also contributes to the development of an environmentally friendly, practical, and scalable adsorbent system. These advancements make CA-BNMG-1 beads an effective and sustainable alternative for water purification applications, with significant advantages over traditional MOF-based systems. The beads demonstrate exceptional Pb(II) adsorption efficiency, consistently achieving over 80% removal across complex aqueous systems containing competing ions and microbial contaminants. Their outstanding selectivity is highlighted by significantly enhanced SFs compared to the parent BNMG-1 MOF, such as an increase in SF(Pb/Mn) from 2.5 to 350, SF(Pb/Ni) from 57.4 to 220.6, and SF(Pb/Cd) from 150.6 to 314. This underscores their strong affinity for Pb(II) over other heavy metals.

The beads also exhibit remarkable structural stability, with minimal Cu(II) leaching, less than 5% at higher and below 1% at lower Pb(II) concentration (5 bead per mL) ensuring environmental safety during application. The ease of separation of the beads from treated water further enhances their practicality for large-scale deployment. Reusability tests confirm that the beads retain over 95% Pb(II) removal efficiency after three cycles, significantly reducing waste and operational costs. By combining green synthesis, high selectivity, stability, and reusability, the CA-BNMG-1 beads provide a scalable, sustainable solution for tackling Pb(II) contamination in water systems, aligning with SSbD framework and promoting environmental stewardship.

This study demonstrates the potential of CA-CuIM beads to remove Pb(II) from complex water matrices, including canal water and artificial seawater. While our findings underscore the importance of coexisting ions and the possible presence of microbes in influencing adsorption behaviour, the quantification and detailed characterization of microbial populations were not performed here. A preliminary result demonstrated >99% bacterial reduction, confirming the strong antibacterial activity on *E. coli* of the CA-BNMG-1 beads (Fig. S6, Section S4†). The antibacterial effect is attributed to Cu leaching, a well-established mechanism where Cu^{2+} ions disrupt bacterial membranes, induce oxidative stress *via* reactive oxygen species (ROS) generation, and inactivate intracellular enzymes, ultimately leading to cell death. To better understand these influences, we have included a table summarising the effects of co-existing organics on Pb(II) removal efficiency of various adsorbent/matrix from the literature, which will inform future work involving coexisting organics and microbial contamination in our system (Table 1).

Future work should include the systematic monitoring of microbial communities in natural water bodies using molecular tools, along with studies focusing on potential synergistic or antagonistic interactions between microbes and the adsorbent under varying environmental conditions. These efforts will not only provide a more comprehensive understanding of adsorption mechanisms but also aid in optimising and expanding the application of CA-CuIM beads for efficient remediation of heavy metal-contaminated waters. Future work will also focus on extending this platform to other heavy metals and contaminants, investigating long-term performance under diverse environmental conditions, and optimising bead synthesis for cost-effective mass production. Exploring hybrid materials and functionalisation strategies could further enhance selectivity and capacity. This scalable and sustainable technology offers a promising pathway toward mitigating heavy metal contamination, supporting environmental health, and advancing green chemistry in water treatment applications.

Data availability

Data are available upon request from the authors.

Author contributions

Prathmesh Bhadane – conceptualisation, methodology, validation, formal analysis, investigation, data curation, writing – original draft, Swaroop Chakraborty –

conceptualisation, methodology, validation, formal analysis, investigation, data curation, writing – original draft, writing – review and editing, funding acquisition.

Conflicts of interest

There are no conflicts to declare.

Acknowledgements

SC acknowledges UKRI NERC Independent Research Fellowship (Grant number – UKRI187), and Engineering and Physical Sciences Research Council Co-Fund [grant number EP/X525662/1] Impact Acceleration Account and the Royal Society International Exchanges grant (IES\R1\241020) for supporting this work. PB expresses gratitude to the Indian Institute of Technology Gandhinagar, India, for awarding the Overseas Research Experience Fellowship (OREF), enabling this research to be conducted at the University of Birmingham, United Kingdom. SC and PB also like to acknowledge Dr. Prateek Goyal, Ms Pankti Dhumal, Prof. Superb Misra, Prof. Abhijit Mishra and Prof. Iseult Lynch for their valuable support during at various phases of this work.

References

1 A. Carmalin Sophia, E. C. Lima, N. Allaudeen and S. Rajan, Application of graphene based materials for adsorption of pharmaceutical traces from water and wastewater- a review, *Desalin. Water Treat.*, 2016, **57**, 27573–27586, DOI: **10.1080/19443994.2016.1172989**.

2 W. S. Chai, J. Y. Cheun, P. S. Kumar, M. Mubashir, Z. Majeed and F. Banat, *et al.*, A review on conventional and novel materials towards heavy metal adsorption in wastewater treatment application, *J. Cleaner Prod.*, 2021, **296**, 126589, DOI: **10.1016/j.jclepro.2021.126589**.

3 B. Tiwari, B. Sellamuthu, Y. Ouarda, P. Drogui, R. D. Tyagi and G. Buelna, Review on fate and mechanism of removal of pharmaceutical pollutants from wastewater using biological approach, *Bioresour. Technol.*, 2017, **224**, 1–12, DOI: **10.1016/j.biortech.2016.11.042**.

4 M. T. Amin, A. A. Alazba and U. Manzoor, A Review of Removal of Pollutants from Water/Wastewater Using Different Types of Nanomaterials, *Adv. Mater. Sci. Eng.*, 2014, **2014**, 1–24, DOI: **10.1155/2014/825910**.

5 D. Paul, Research on heavy metal pollution of river Ganga: A review, *Ann. Agric. Sci.*, 2017, **15**, 278–286, DOI: **10.1016/j.aasci.2017.04.001**.

6 X. Han, H. Wu, Q. Li, W. Cai and S. Hu, Assessment of heavy metal accumulation and potential risks in surface sediment of estuary area: A case study of Dagu river, *Mar. Environ. Res.*, 2024, **196**, 106416, DOI: **10.1016/j.marenvres.2024.106416**.

7 B. Prasad Ahirvar, P. Das, V. Srivastava and M. Kumar, Perspectives of heavy metal pollution indices for soil, sediment, and water pollution evaluation: An insight, *Total Environ. Res. Themes*, 2023, **6**, 100039, DOI: **10.1016/j.totert.2023.100039**.

8 K. Raj and A. P. Das, Lead pollution: Impact on environment and human health and approach for a sustainable solution, *Environ. Chem. Ecotoxicol.*, 2023, **5**, 79–85, DOI: **10.1016/j.enceco.2023.02.001**.

9 V. Kumar, S. K. Dwivedi and S. Oh, A critical review on lead removal from industrial wastewater: Recent advances and future outlook, *J. Water Process Eng.*, 2022, **45**, 102518, DOI: **10.1016/j.jwpe.2021.102518**.

10 S. Wang, H. Wang, S. Wang, L. Fu and L. Zhang, Novel magnetic covalent organic framework for the selective and effective removal of hazardous metal Pb(II) from solution: Synthesis and adsorption characteristics, *Sep. Purif. Technol.*, 2023, **307**, 122783, DOI: **10.1016/j.seppur.2022.122783**.

11 H. Wang, S. Wang, S. Wang, L. Fu and L. Zhang, Efficient metal-organic framework adsorbents for removal of harmful heavy metal Pb(II) from solution: Activation energy and interaction mechanism, *J. Environ. Chem. Eng.*, 2023, **11**, 109335, DOI: **10.1016/j.jece.2023.109335**.

12 M. R. Awual, An efficient composite material for selective lead(II) monitoring and removal from wastewater, *J. Environ. Chem. Eng.*, 2019, **7**, 103087, DOI: **10.1016/j.jece.2019.103087**.

13 A. Shahat, H. M. A. Hassan, H. M. E. Azzazy, E. A. El-Sharkawy, H. M. Abdou and M. R. Awual, Novel hierarchical composite adsorbent for selective lead(II) ions capturing from wastewater samples, *Chem. Eng. J.*, 2018, **332**, 377–386, DOI: **10.1016/j.cej.2017.09.040**.

14 P. Bhadane and A. Mishra, Versatile, flexible rice starch–graphene oxide bio-nanocomposites, *Environ. Sci.: Water Res. Technol.*, 2024, **10**, 2432–2441, DOI: **10.1039/D4EW00419A**.

15 M. S. Aljohani, R. B. Alnoman, H. Y. Alharbi, M. Al-Anazia and M. Monier, Designing of a cellulose-based ion-imprinted biosorbent for selective removal of lead (II) from aqueous solutions, *Int. J. Biol. Macromol.*, 2024, **259**, 129145, DOI: **10.1016/j.ijbiomac.2023.129145**.

16 X. Guo, T. Wang, F. Yang, H. Xu, C. Mu and W. Ye, *et al.*, Selective removal and monitoring of Pb(II) ions in wastewater using fluorescence-enhanced silicon quantum dot composites, *Sep. Purif. Technol.*, 2025, **359**, 130666, DOI: **10.1016/j.seppur.2024.130666**.

17 S. Chakraborty, D. Menon, I. Mikulska, C. Pfrang, D. Fairen-Jimenez, S. K. Misra and I. Lynch, Make metal–organic frameworks safe and sustainable by design for industrial translation, *Nat. Rev. Mater.*, 2025, **10**, 167–169, DOI: **10.1038/s41578-025-00774-6**.

18 C. Apel, K. Kümmerer, A. Sudheshwar, B. Nowack, C. Som and C. Colin, *et al.*, Safe-and-sustainable-by-design: State of the art approaches and lessons learned from value chain perspectives, *Curr. Opin. Green Sustainable Chem.*, 2024, **45**, 100876, DOI: **10.1016/j.cogsc.2023.100876**.

19 L. G. Soeteman-Hernández, C. Apel, B. Nowack, A. Sudheshwar, C. Som and E. Huttunen-Saarivirta, *et al.*, The safe-and-sustainable-by-design concept: innovating towards a more sustainable future, *Environ. Sustainability*, 2024, **7**, 363–368, DOI: **10.1007/s42398-024-00324-w**.

20 P. Dhumal, S. Chakraborty, B. Ibrahim, M. Kaur and E. Valsami-Jones, Green-synthesised carbon nanodots: A SWOT

analysis for their safe and sustainable innovation, *J. Cleaner Prod.*, 2024, **480**, 144115, DOI: 10.1016/j.jclepro.2024.144115.

21 I. Furxhi, A. Costa, S. Vázquez-Campos, C. Fito-López, D. Hristozov and J. A. Tamayo Ramos, *et al.*, Status, implications and challenges of European safe and sustainable by design paradigms applicable to nanomaterials and advanced materials, *RSC Sustainability*, 2023, **1**, 234–250, DOI: 10.1039/D2SU00101B.

22 R. Freund, O. Zaremba, G. Arnauts, R. Ameloot, G. Skorupskii and M. Dincă, *et al.*, The Current Status of MOF and COF Applications, *Angew. Chem., Int. Ed.*, 2021, **60**, 23975–24001, DOI: 10.1002/anie.202106259.

23 L. Rani, J. Kaushal, A. L. Srivastav and P. Mahajan, A critical review on recent developments in MOF adsorbents for the elimination of toxic heavy metals from aqueous solutions, *Environ. Sci. Pollut. Res.*, 2020, **27**, 44771–44796, DOI: 10.1007/s11356-020-10738-8.

24 F. Ahmadijokani, A. Ghaffarkhah, H. Molavi, S. Dutta, Y. Lu and S. Wuttke, *et al.*, COF and MOF Hybrids: Advanced Materials for Wastewater Treatment, *Adv. Funct. Mater.*, 2024, **34**, 2305527, DOI: 10.1002/adfm.202305527.

25 N. C. Burtch, H. Jasuja and K. S. Walton, Water Stability and Adsorption in Metal–Organic Frameworks, *Chem. Rev.*, 2014, **114**, 10575–10612, DOI: 10.1021/cr5002589.

26 P. Goyal, A. Paruthi, D. Menon, R. Behara and A. Jaiswal, *et al.*, Fe doped bimetallic HKUST-1 MOF with enhanced water stability for trapping Pb(II) with high adsorption capacity, *Chem. Eng. J.*, 2022, **430**, 133088, DOI: 10.1016/j.cej.2021.133088.

27 A. Domán, O. Czakkel, L. Porcar, J. Madarász, E. Geissler and K. László, Role of water molecules in the decomposition of HKUST-1: Evidence from adsorption, thermoanalytical, X-ray and neutron scattering measurements, *Appl. Surf. Sci.*, 2019, **480**, 138–147, DOI: 10.1016/j.apsusc.2019.02.177.

28 S. Chakraborty, B. Ibrahim, P. Dhumal, N. Langford, L. Garbett and E. Valsami-Jones, Perturbation of enzyme structure by nano-metal organic frameworks: A question mark on their safety-by-design?, *J. Hazard. Mater. Lett.*, 2024, **5**, 100127, DOI: 10.1016/j.hazl.2024.100127.

29 P. Dhumal, P. Bhadane, B. Ibrahim and S. Chakraborty, Evaluating the path to sustainability: SWOT analysis of safe and sustainable by design approaches for metal–organic frameworks, *Green Chem.*, 2025, **27**, 3815–3850, DOI: 10.1039/D5GC00424A.

30 G. Zhi, X. Qi, Y. Li, J. Wang and J. Wang, Efficient treatment of smelting wastewater: 3D nickel foam @MOF shatters the previous limitation, enabling high-throughput selective capture of arsenic to form non-homogeneous nuclei, *Sep. Purif. Technol.*, 2024, **328**, 124927, DOI: 10.1016/j.seppur.2023.124927.

31 P. Bhadane, P. Mahato, D. Menon, B. K. Satpathy, L. Wu and S. Chakraborty, *et al.*, Hydrolytically stable nanosheets of Cu–imidazolate MOF for selective trapping and simultaneous removal of multiple heavy metal ions. Environ Sci, *Nano*, 2024, **11**, 2385–2396, DOI: 10.1039/D3EN00754E.

32 P. Bhadane, D. Menon, P. Goyal, M. Reza Alizadeh Kiapi, B. Kanta Satpathy and A. Lanza, *et al.*, A two-dimensional metal-organic framework for efficient recovery of heavy and light rare earth elements from electronic wastes, *Sep. Purif. Technol.*, 2025, **360**, 130946, DOI: 10.1016/j.seppur.2024.130946.

33 P. Bhadane and S. Chakraborty, Cross-material synergies of carbon nanomaterials, MOFs, and COFs: Innovative approaches for sustainable environmental remediation and resource recovery, *Coord. Chem. Rev.*, 2025, **535**, 216669, DOI: 10.1016/j.ccr.2025.216669.

34 P. Butreddy, S. Chakraborty, P. Soppina, R. Behera, V. Soppina and S. K. Misra, Novel dual labelled nanoprobes for nanosafety studies: Quantification and imaging experiment of CuO nanoparticles in C. elegans, *Chemosphere*, 2022, **286**, 131698, DOI: 10.1016/j.chemosphere.2021.131698.

35 M. F. Navarro Poupard, E. Polo, P. Taboada, A. Arenas-Vivo, P. Horcajada and B. Pelaz, *et al.*, Aqueous Synthesis of Copper(II)-Imidazolate Nanoparticles, *Inorg. Chem.*, 2018, **57**, 12056–12065, DOI: 10.1021/acs.inorgchem.8b01612.

36 M. Kamal, E. M. Abdelrazek, N. M. Sellow and A. M. Abdelghany, Synthesis and optimization of Novel Chitosan/Cellulose Acetate Natural Polymer Membrane for water treatment, *J. Adv. Phys.*, 2018, **14**, 5303–5311, DOI: 10.24297/jap.v14i1.7183.

37 K. Fu, Y. Zhang, H. Liu, C. Lv, J. Guo and J. Luo, *et al.*, Construction of metal-organic framework/polymer beads for efficient lead ions removal from water: Experiment studies and full-scale performance prediction, *Chemosphere*, 2022, **303**, 135084, DOI: 10.1016/j.chemosphere.2022.135084.

38 C. Zhang, W. Chen, G. Owens and Z. Chen, Recovery of rare earth elements from mine wastewater using alginate microspheres encapsulated with zeolitic imidazolate framework-8, *J. Hazard. Mater.*, 2024, **471**, 134435, DOI: 10.1016/j.jhazmat.2024.134435.

39 Q. Qin, Q. Wang, D. Fu and J. Ma, An efficient approach for Pb(II) and Cd(II) removal using manganese dioxide formed in situ, *Chem. Eng. J.*, 2011, **172**, 68–74, DOI: 10.1016/j.cej.2011.05.066.

40 A. A. Qaiser, M. M. Hyland and D. A. Patterson, Surface and Charge Transport Characterization of Polyaniline–Cellulose Acetate Composite Membranes, *J. Phys. Chem. B*, 2011, **115**, 1652–1661, DOI: 10.1021/jp109455m.

41 J. Nonkumwong, S. Ananta and L. Srisombat, Effective removal of lead(II) from wastewater by amine-functionalized magnesium ferrite nanoparticles, *RSC Adv.*, 2016, **6**, 47382–47393, DOI: 10.1039/C6RA07680G.

42 M. Sekar, V. Sakthi and S. Rengaraj, Kinetics and equilibrium adsorption study of lead(II) onto activated carbon prepared from coconut shell, *J. Colloid Interface Sci.*, 2004, **279**, 307–313, DOI: 10.1016/j.jcis.2004.06.042.

43 M. Momčilović, M. Purenović, A. Bojić, A. Zarubica and M. Ranđelović, Removal of lead(II) ions from aqueous solutions by adsorption onto pine cone activated carbon, *Desalination*, 2011, **276**, 53–59, DOI: 10.1016/j.desal.2011.03.013.

44 M. R. Lasheen, I. Y. El-Sherif, D. Y. Sabry, S. T. El-Wakeel and M. F. El-Shahat, Removal of heavy metals from aqueous solution by multiwalled carbon nanotubes: equilibrium, isotherms, and kinetics, *Desalin. Water Treat.*, 2015, **53**, 3521–3530, DOI: 10.1080/19443994.2013.873880.

45 S. Chakraborty, P. Dhumal, Z. Guo, M. L. Gifford and I. Lynch, From soil to table: How safe and sustainable by design MOFs can revolutionize agriculture and food security, *Matter*, 2025, 102095, DOI: **10.1016/j.matt.2025.102095**.

46 Y. Wang, S. Liang, B. Chen, F. Guo, S. Yu and Y. Tang, Synergistic Removal of Pb(II), Cd(II) and Humic Acid by Fe3O4@Mesoporous Silica-Graphene Oxide Composites, *PLoS One*, 2013, **8**, e65634, DOI: **10.1371/journal.pone.0065634**.

47 S. Biswas, A. K. Nayak and A. Pal, Surfactant-influenced biosorption as a sustainable and effective way for the eradication of environmental pollutants: a review, *RSC Sustainability*, 2025, **3**, 112–133, DOI: **10.1039/d4su00574k**.

48 C. Song, J. Liu, L. Zhang, J. Wang and X. Shu, Competitive Adsorption of Pb2+ from Aqueous Solutions by Multi-Source Lignocellulose-Derived Hydrothermal Humic Acid, *Processes*, 2025, **13**, 155, DOI: **10.3390/pr13010155**.

49 Y. Jiang, Z. Qin, J. Fei, D. Ding, H. Sun and J. Wang, *et al.*, Surfactant-induced adsorption of Pb(II) on the cracked structure of microplastics, *J. Colloid Interface Sci.*, 2022, **621**, 91–100, DOI: **10.1016/j.jcis.2022.04.068**.